Front. Chem. Sci. Eng. 2020, 14(6): 1087–1099
https://doi.org/10.1007/s11705-019-1895-z

RESEARCH ARTICLE

High-gravity-assisted emulsification for continuous preparation of waterborne polyurethane nanodispersion with high solids content

Weihong Zhang[1,2], Dan Wang (✉)[1], Jie-Xin Wang[1,2], Yuan Pu (✉)[2], Jian-Feng Chen[1,2]

1 State Key Laboratory of Organic-Inorganic Composites, Beijing University of Chemical Technology, Beijing 100029, China
2 Research Centre of the Ministry of Education for High Gravity Engineering and Technology, Beijing University of Chemical Technology, Beijing 100029, China

Abstract In this work, we developed a continuous preparation strategy for the production of high-solids-content waterborne polyurethane (WPU) emulsions via high-gravity-assisted emulsification in a rotating packed bed (RPB) reactor. By adjusting the experimental parameters and formula, WPU emulsions with a high solids content of 55% and a low viscosity were prepared. Preliminary applications of the high-solids-content WPU as a thermally insulating material were demonstrated. RPB emulsification is an economical and environmentally friendly production strategy because of the low energy consumption, short emulsification time, and effective devolatilization. This study demonstrated an effective method for preparation of high-solids-content WPU, moving toward commercialization and industrialization.

Keywords waterborne polyurethane, rotating packed bed, emulsification, nanodispersion, high solids content

1 Introduction

In the previous decade, various products consisting of volatile organic compound-free polymers, which are considered a class of green materials, have been created for use in coatings [1], adhesives [2], multi-functional materials [3], and others [4,5]. Waterborne polyurethane (WPU) dispersions have recently attracted increased attention because of their excellent chemical and mechanical properties and their suitability with respect to environmental requirements and human health [6]. It is noteworthy that hydrophilic monomers, include carboxylate, sulfonate, quaternary ammonium salts, or non-ionic groups, are usually embedded into the molecular chain to obtain self-emulsification and good stability of the dispersions in water [7]. To date, anionic WPUs are commercially predominant and carboxylates, especially dimethyl propionic acid (DMPA), are the most common products reported in the literature [8–11]. However, commercial WPU products generally exhibit low solids contents, which lead to a slow drying rate, high latent heat consumption, and high transport costs; therefore, the preparation of high-solids-content WPU is of industrial significance [12].

The key point for preparation of WPU with high solids content is to effectively disperse polyurethane pre-polymers into water to form a stable colloidal dispersion. However, a high solids content and high viscosity often occur simultaneously. As the solids content of WPU increases to over 45%, the emulsion viscosity usually increases sharply because of the swelling of WPU particles and the strong interactions between neighboring particles. Theoretically, particles of WPU can be regarded as balls with nanoscale diameters, with a classical structure consisting of a hydrophobic core, water-swelling layer, and electric double layers [13]. The electro viscous effect caused by the existence of the electric double layer can be considered to lead to the increasing viscosity [14]. Mathematical models describe the limitation of solids content for monodispersed dispersions: The viscosity will approach infinity as the volume fraction approaches 0.64, which can be identified as the upper limit of solids content [15]. The relationship among the solids content, particle size distribution (PSD), and apparent viscosity (η) is key to achieving a high solids content and low viscosity at the same time. It is easy to explain that over a wide range of diameters, some small particles can fill into the interstitial

Received July 21, 2019; accepted August 22, 2019

E-mails: wangdan@mail.buct.edu.cn (Wang D), puyuan@mail.buct.edu.cn (Pu Y)

gaps between larger ones [16]. Using the PSD theory, many efforts have been taken to achieve preparation of WPU with high solids content, including physical blending to mix two kinds of WPU emulsions with different size distributions and achieve a bimodal size distribution [6,13], or combining various hydrophilic monomers in different position of the WPU chains [17–19]. The extension of these laboratory technologies or strategies into mass production of WPU has been limited because of the complicated processes. In addition, according to the analysis of the emulsification process, there is a critical point in the typical phase inversion emulsification process where it becomes uncontrollable and unstable [20]. During the emulsification, the dispersion in the system is heterogeneous, which can cause problems. The water added into the pre-polymer phase often exceeds the phase inversion limit and causes the production of low-solids-content emulsions [21]. Meanwhile, emulsification will be terminated because of the high viscosity resulting from the addition of small amounts of water [22].

A high-gravity-assisted rotating packed bed (RPB) reactor has been developed as an efficient apparatus that provides strong centrifugal acceleration, which can enhance interphase mass transfer by one to three orders of magnitude compared with the conventional stirring reactor [23,24]. The high-gravity technique shows advantages in the synthesis of nanoparticles [25,26], nanodispersions [27], and emulsions [28]. Conventional methods for preparation of emulsions, such as mechanical stirring, homogenization, sonication, and phase inversion emulsification, are difficult to scale up and present a challenge in producing WPU emulsions with high solids contents [29,30].

Herein, based on the use of a RPB reactor, we developed a high-gravity-assisted emulsification strategy to realize the two-step continuous production of high-solids-content WPU emulsions. The cycle time and high-gravity levels were investigated to achieve controllable preparation. Other advantages of RPB emulsification are discussed, including emulsifying time, devolatilization, and fine dispersibility [24]. The high-gravity emulsification strategy provides a new platform for preparation of high-solids-content WPU emulsions that can potentially be applied for large-scale industrial production.

2 Experimental

2.1 Materials

Diphenyl-methane-diisocyanate (MDI), poly(propylene glycol) (PPG, M_W = 2000), 1,4-butane diol (BDO), DMPA, and triethylamine (TEA) were purchased from Aladdin Industrial Corporation. Acetone was purchased from Vas Chemical Reagent Corp. (Beijing, China). BDO and PPG were dried under vacuum at 120°C for 8 h before use; acetone was distilled and kept in a 4-Å molecular sieve before use. All chemicals were used without any additional purification unless specifically mentioned, and deionized water was used for all experiments.

2.2 Synthesis strategy for WPU dispersion

A condenser, a mechanical stirrer, and a thermometer were installed in a 500-mL round-bottomed, four-necked flask equipped with a N_2 atmosphere inlet. DMPA and PPG-2000 were first decanted and mixed well at 110°C for 30 min to remove trace water from the raw material. The pre-polymerization reaction occurred for 3 h, beginning with the addition of MDI to the flask at 60°C. The hydrophilic groups were introduced in polyisocyanate chains. Then, BDO was added to the flask at 60°C; the reactions were implemented at 60°C until the theoretical –NCO values were obtained, as determined by the dibutylamine titration method (ASTM D2572-97(2010)). The mixture was cooled to 45°C. Then, TEA was added and the neutralization reaction proceeded for 40 min. Acetone (15 wt-%) was added to reduce the viscosity. The entire reaction is shown in Scheme 1.

2.3 Emulsification in RPB reactor

Emulsification was conducted in the RPB reactor. The pre-polymer was cooled to 25°C, after which the pre-polymer and distilled water (based on various solids contents, cooled before used) were pumped into an RPB reactor via two peristaltic pumps at a set liquid flow rate. The WPU emulsion was collected from the liquid outlet and pumped into the RPB reactor in a circulatory manner until the viscosity of the WPU emulsion decreased macroscopically. It is easy to explain why the swelling effect of the particles was reduced, as the acetone was removed from the emulsion assisted by the devolatilization from the RPB reactor. The removed acetone was cooled and recycled in the polymerization process. The high-gravity levels were controlled by adjusting the rotation speeds of the RPB in the range of 17–50 Hz, which converts to a range of 969–2850 revolutions per minute (rpm). The external circulation RPB reactor was used, where the kernel component of the RPB reactor is a rotator filled with 2.5-cm-thick stainless packing; more details about the RPB reactor can be found in a previous report [31]. The high-gravity levels were calculated using the following equation [32]:

$$\beta = \frac{\int_{r_1}^{r_2} 2\pi r \beta \mathrm{d}r}{\int_{r_1}^{r_2} 2\pi r \mathrm{d}r} = \frac{2\omega^2(r_1^2 + r_1 r_2 + r_2^2)}{3(r_1 + r_2)g}, \quad (1)$$

where r_1 and r_2 are the inner and outer radius of packing (m), and ω is the rotor speed (rad·s^{-1}).

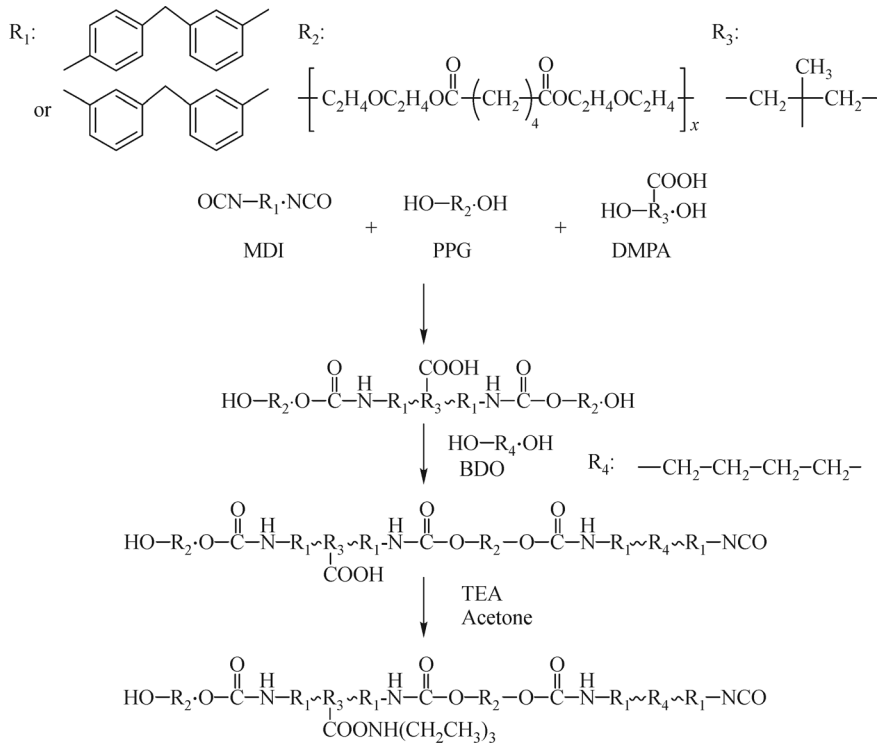

Scheme 1 Preparation process of MDI-WPU.

2.4 Characterization

The zeta potential and PSD of the particles in water were determined by a Malvern Zetasizer Nano ZS90 instrument via electrophoretic light scattering and dynamic light scattering (DLS) at 25°C, respectively. The samples were diluted to 5 mg·mL^{-1} before the particle size analysis. Each sample was measured three times, and at least 12 runs were performed for each measurement. The viscosity of the WPU dispersions was measured in a Brookfield digital viscometer (Modal DV-III). Measurement was carried out at 25°C. The solids content of the WPU was detected by drying the emulsion at 110°C for 3 h and calculating the weight ratio of the residue to the emulsion. The exact value of the solids content was measured until the data were stable. The stability of the high-solids-content WPU emulsion was tested by drying in an oven at 50°C and observing the condition every day until precipitation occurred. The sample was analyzed using a Hitachi HT7700 transmission electron microscope (TEM) at an accelerating voltage of 100 kV. Configuration phosphotungstic acid solution with a mass fraction of 0.02. The WPU water dispersions were diluted with deionized water until the mass fraction was 0.003 to 0.007. Then, 2 mL of each solution was mixed and negative stained for 1 min, then dropped on a copper grid and air-dried at room temperature before observation. Nano Measurer was used to obtain histograms of the PSD.

3 Results and discussion

The WPU emulsion was prepared using a multi-step strategy. Step one was the classical preparation of WPU. Step two was high-gravity-assisted emulsification, which has been rarely studied; the mechanism is different from that of conventional stirred tank reactors (STR). The appearance of a phase inversion point between the oil phase and water phase in emulsification is inevitable during conventional STR reactor emulsification operation. The RPB reactor has a specific design structure, shown in Fig. 2. Deionized water and the pre-polymer were injected into the packed bed through the nozzle with a set kinetic energy from the feed pump at a set ratio. The polyurethane pre-polymer and deionized water collide and mix in the form of droplets; then, the liquids are reduced into micron or nanometer-size droplets after jetting to the high-speed rotating wire mesh packing. This process increases the nano-sized mixture and dispersion. Also, in this emulsification process, the residual –NCO of the pre-polymer eventually forms urea and biuret derivatives after reacting with water.

In research regarding the formulation, all the components used in the process of WPU production, like diisocyanates, polyols, hydrophilic monomers, and neutralizers, play a significant role. However, it is also difficult to explain all the effects of the various components, as contradictory results are often reported in the literature,

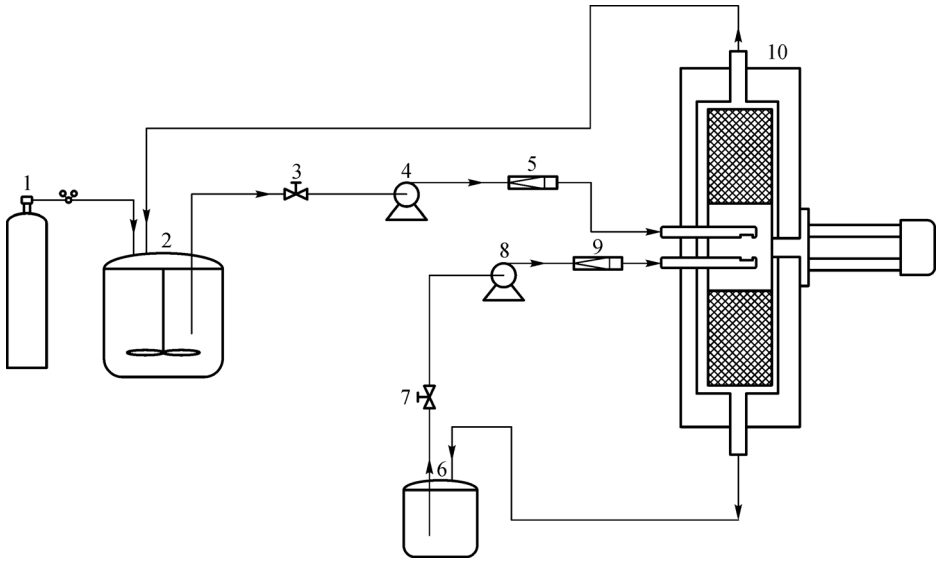

Fig. 1 Schematic diagram of experimental setup for WPU emulsification. 1: Nitrogen cylinder; 2: pre-polymerization reactor; 3, 7: valve; 4, 8: pump; 5, 9: flow meter; 6: emulsion storage tank; 10: RPB.

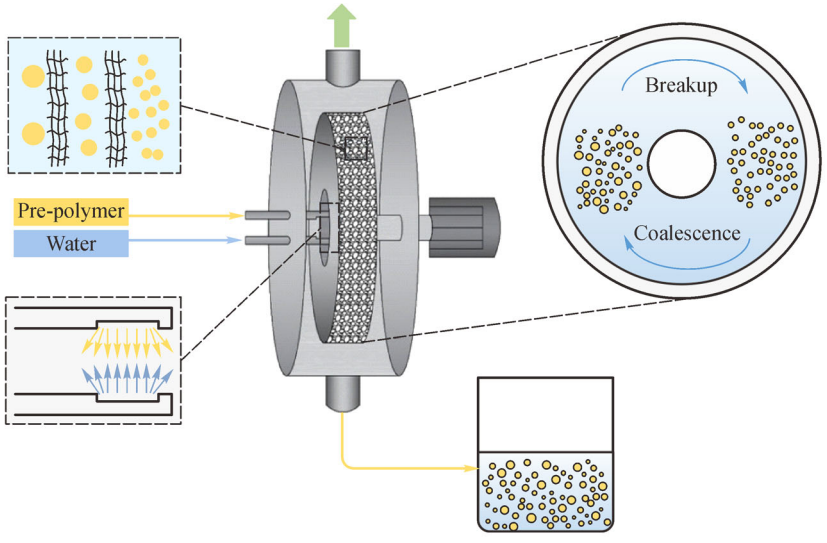

Fig. 2 Specific design structure of the RPB reactor.

making comparisons between two studies difficult [33]. The purpose of our experiment was to attempt to use a normalized and inexpensive formulation and attain a continuous emulsification with an industrially relevant method. Research on WPU formulation and application was simplified, and the isocyanate index (R value) and DMPA mass fraction are discussed with respect to the influence of emulsion quality and the difficulty of emulsification operation. Theoretically, the size of the WPU particles is closely related to the content of the hydrophilic monomers. The surface charge density of emulsion particles corresponds to the similar ζ potentials in water, to enable stable dispersion in water. Thus, a particle containing a low amount of hydrophilic monomer requires the aggregation of more WPU chains to attain a sufficient charge density, making the WPU particles larger in size. Conversely, one containing a higher amount of hydrophilic monomer has a smaller size. During polymerization, the isocyanate and the polyol proceed with a one-to-one polymerization, and the R value indicates the degree of excess isocyanate; the amount of the –NCO group remaining affects the molecular weight of the polyurethane pre-polymer. The small R value (1.05–1.2) indicates a higher molecular weight and longer molecular chain, which also causes difficulty in feeding. Furthermore, a large R value means that a large amount of –NCO groups

were unreacted, so they can react with water during the emulsification and produce a large amount of polyurea, which affects dispersion in the RPB packing.

During the emulsification process, competition between the reaction and dispersion of pre-polymer affects the outcome of emulsification. When the pre-polymer mixing process is dominated by dispersion, the growth of the molecular chain can be regarded as occurring inside the WPU particles, forming a stable emulsion system with a small PSD. When the chain extension reaction dominates, the highly reactive isocyanate group produces polyurea with a strong hydrogen bonding and covers the surface of the pre-polymer, which leads to difficulty in dispersion. To our knowledge, excessive stirring speed cannot further strengthen the dispersion process. However, the dispersion time can be further increased in the RPB reactor, and a short dispersion time could avoid the formation of polyurea in the RPB packing before dispersion, which would also prevent the failure of emulsification. Therefore, analysis of dispersion in the RPB reactor is performed. Figure 3 shows a sketch of emulsification in the RPB environment, which can be considered a two-step mixing process where the pre-polymer is gradually stirred into the circulating water first (Fig. 3(a)), after which the two flows are pump into the RPB and emulsification is complete after a certain circulation time (Fig. 3(d)). Figures 3(c) and 3(f) show the influence of the pre-polymer flow rate and circulating flow rate on the Z-average size during the RPB emulsification process; the magnitude of the flow rate was recorded and is quantified by the numbers displayed, which indicate the rotation speed of the peristaltic pump, where the units of flow rate are rpm. In Fig. 3(c), the pre-polymer flow rate was identified as an independent variable changing from 50 to 200 rpm, and the flow rate of circulating material remained at 150 rpm for the entire experiment. When the pre-polymer flow rate was 50 rpm, the Z-average size was 129.9 nm, and as the pre-polymer flow rate was increased to 200 rpm, the Z-average first decreased to 74.13 nm and then increased as the pre-polymer flow rate exceeded 100 rpm. It can be deduced that at a low flow rate, it was difficult for the pre-polymer to form a jet flow at the feed nozzle, which caused worse dispersion; this result is also simulated by computational fluid dynamics (CFD) and shown at the top of Fig. 3(b). When the pre-polymer flow rate was increased to 100 rpm, the liquid at the feed port was sprayed to a jet flow, which

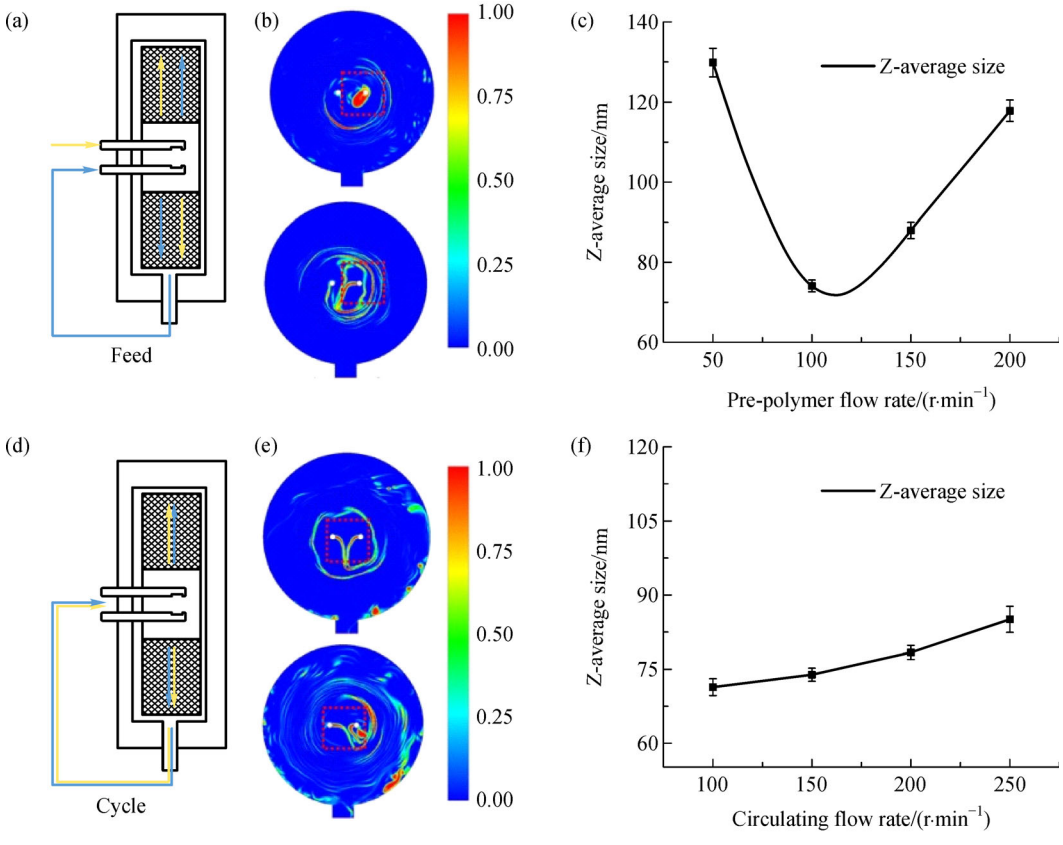

Fig. 3 (a) Sketch of the first step of the mixing process in the RPB; (b) the liquid flow distribution simulated by CFD with respect to the pre-polymer flow rate at 50 and 100 rpm; (c) the Z-average size obtained with various pre-polymer flow rates; (d) sketch of the second step of the mixing process in the RPB; (e) the liquid flow distribution simulated by CFD with respect to the circulating flow rate at 100 and 250 rpm; (f) the Z-average size obtained with various circulating flow rates.

led to a sufficient dispersion, as illustrated at the bottom of Fig. 3(b). With a further increase in the flow rate, the partial pre-polymer was in excess and the dispersion time increased, which dominated the reaction and led to an increased Z-average size. The top and bottom of the CFD simulation diagram in Fig. 3(e) shows the liquid flow distribution when the circulating flow rate was 100 and 250 rpm, respectively, and Fig. 3(f) shows the influence of circulating flow rate on the Z-average size. As the circulating flow rate increased, the Z-average size also showed a small increase. This result means that the RPB reactor has a high operational upper limit. However, considered the flooding of WPU foam, the optimum circulating flow rate was 150 rpm.

A series of experiments was carried out to investigate how the number of cycles and high-gravity level influence the Z-average size and polydispersity index (PDI) of WPU emulsion, which can indirectly influence the solids content of the WPU emulsion. The number of cycles is a parameter used to measure the number of times in which the emulsion system was completely exposed to the high-gravity environment and can be considered as an indicator of emulsification time. The completion of one cycle of emulsions was recorded as one cycle, and the number of cycles can be obtained by dividing the emulsification time by one cycle time. The effect of the number of cycles on size distribution and PDI is shown in Fig. 4. The emulsions obtained at various numbers of cycles were analyzed by DLS measurements. The number of cycles of RPB has a significant influence on the size and size distribution. As the number of cycles increases, the size distribution first narrows and then becomes broad. In the experimental range, 45 cycles results in a narrow size distribution, and a broad size distribution occurs when the number of cycles is 90 (Fig. 4(a)). The Z-average size and PDI change at various cycle times is demonstrated in Fig. 4(b), which shows that as the number of cycles changed from 15 to 45, the particle size of the WPU emulsion decreased from approximately 89 to 70 nm. Throughout this process, the PDI of the WPU emulsion also decreased, from approximately 0.115 to 0.095. As the number of cycles increased from 45 to 90, the particle size of the emulsion also increased, from 70 to 80 nm, and the PDI increased from 0.095 to 0.320. Figure 4(c) shows a typical size distribution contrast for 45 cycles in a RPB reactor and in a STR reactor, where the size distribution has a distinctly wider trend; this results clearly demonstrates that adjusting the number of cycles is a possible method for controlling the PSD.

The effect of high-gravity level on size distribution and PDI is shown in Fig. 5. The size and size distribution were analyzed by DLS measurements as the high-gravity level

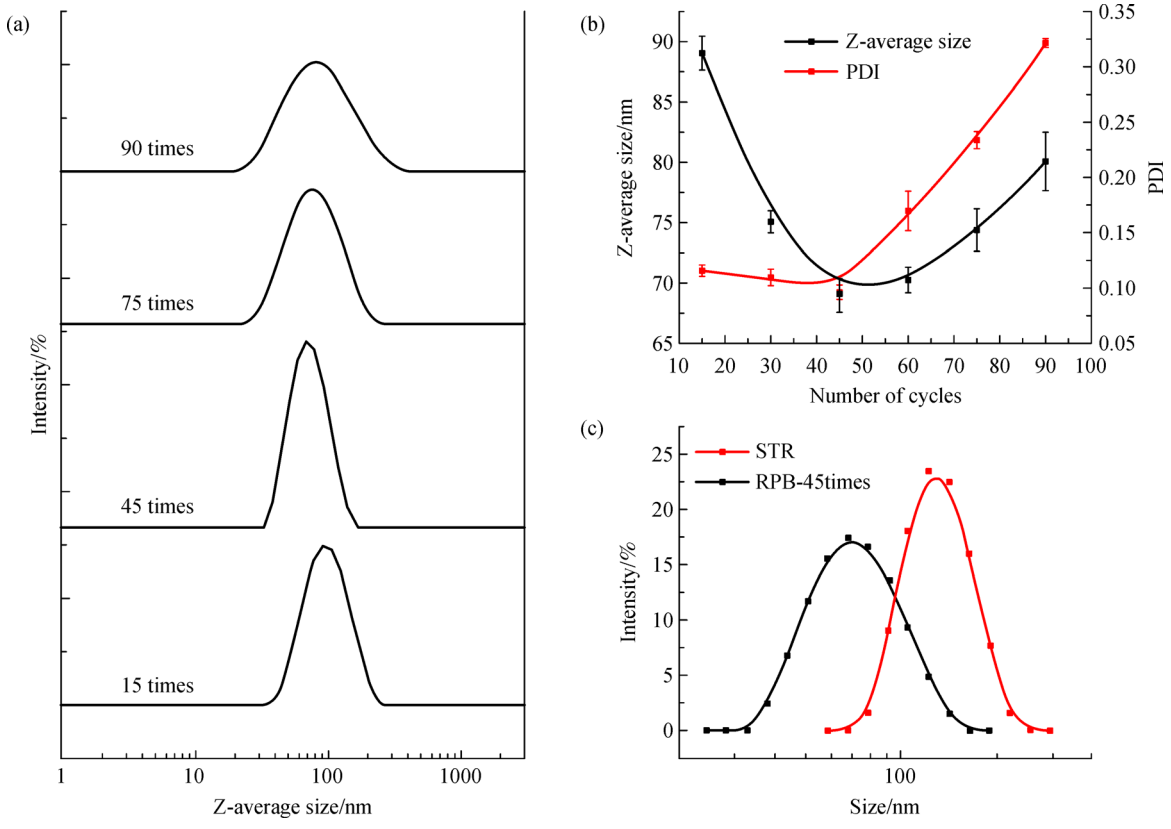

Fig. 4 (a) Particle sizes distribution of WPU particles obtained after various numbers of cycles; (b) the Z-average size and PDI of WPU particles obtained after various numbers of cycles; (c) the contrast in PSD between 45 cycles in the RPB and STR reactors.

was varied from 50 to 430. Figure 5(a) presents the PSD change for the various high-gravity levels, where the PSD became broad as the high-gravity level increased. When the high-gravity level was up to 430, the PSD became bimodal, and the percentage of large particles was much greater than that of small ones. According to previous research, when the volume percentage of large particles is greater than 70%, small particle can fill the interstices between large particles, and the WPU emulsion can exhibit a lower viscosity and a higher solids content [34]. Therefore, our results show that it is viable to obtain a broad PSD using the RPB reactor to reach a high solids content. Figure 5(b) shows that as the high-gravity levels changed from 50 to 135, the Z-average size and PDI decreased because of the increased shear force. At high high-gravity levels, the Z-average size of WPU particles is positively correlated with the high-gravity level, as is PDI. In addition, emulsification using the STR can result in a medium Z-average of the WPU particles (103.9 nm) and a high PDI (0.346). Compared with the STR, the RPB reactor can produce particles with a smaller Z-average and low PDI when the high-gravity level is in the appropriate range. This result means that using the RPB reactor, it is possible to produce a uniform WPU emulsion, which has a smaller size and PDI than conventional emulsification. Figure 5(c) compares typical size distributions of the 430*g* and STR reactors, where it is clear that adjusting the high-gravity level is a key factor in controlling the PSD.

Figure 6 shows TEM photographs of WPU under various experimental RPB parameters. Figures 6(a) and 6 (b) are for high-gravity levels of 50 and 135, respectively, showing a marked change in PSD, which is also suggested by the DLS data. Comparing Fig. 6(c) and Fig. 6(d), it is clear that the number of cycles significantly affects the PSD. As the number of cycles increases, the PSD becomes broad.

Several reports have pointed out that a RPB reactor provides a strong shear-force environment by the wire mesh packing, which can split the pre-polymer into smaller sizes. Meanwhile, the shear effects intensify as the rotation speed increases, so it can be inferred that increasing the high-gravity level (rotation speed) can enhance the shear effects and lead to a small average particle size. However, the shear effect is restricted by the content of the hydrophilic monomers, as discussed above. As Fig. 7 shows, there is another effect in the RPB environment that we can call coalescence: Small particles can coalesce with one another to form a larger one. There are many reports showing that emulsified droplets will coalesce under a centrifugal field [35]. This coalescence will cause flocculation and sedimentation and is often considered a factor leading to destabilization of the emulsion. Surpris-

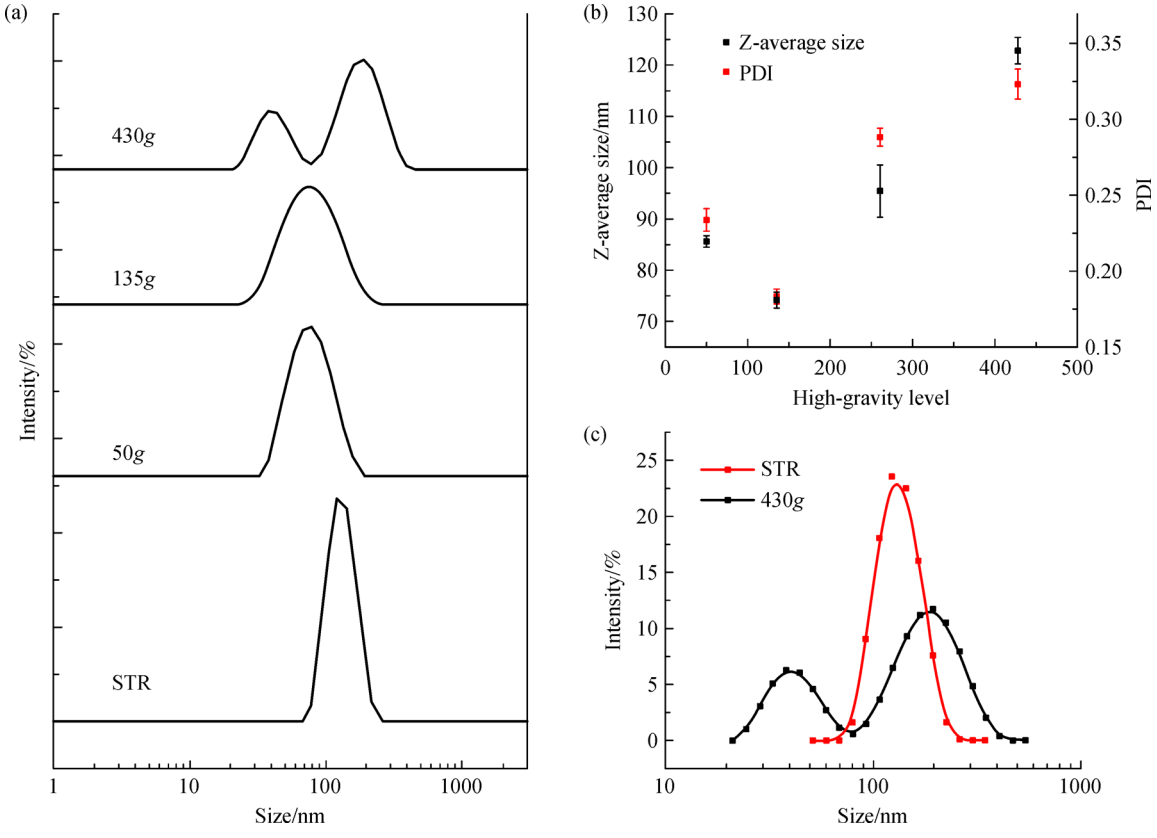

Fig. 5 (a) PSD of WPU particles obtained at various high-gravity levels; (b) the Z-average size and PDI of WPU particles obtained at various high-gravity levels; (c) the comparison of PSDs between STR and RPB with 430*g*.

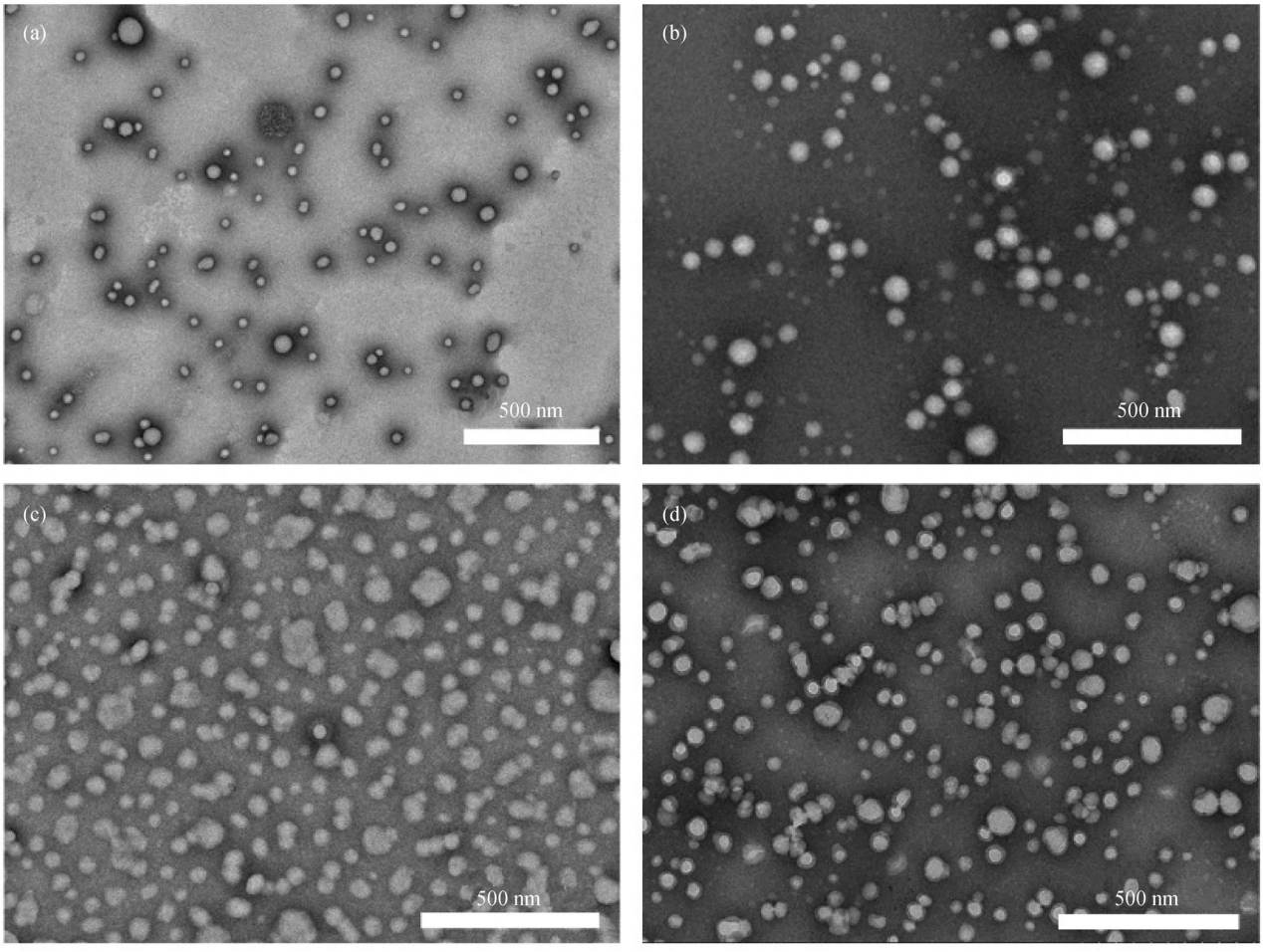

Fig. 6 (a) TEM image of WPU for 50*g*; (b) TEM image of WPU for 135*g*; (c) TEM image of WPU after 15 cycles; (d) TEM image of WPU after 75 cycles.

ingly, the RPB provides a strong centrifugal acceleration and a large shear force environment at the same time, where the two opposing effects will be in equilibrium. The coalescence plays a significant role in the determination of size evolution and WPU size distribution. To coalesce, the particles must have sufficient kinetic energy to overcome the barrier potential, which indicates that the increasing rpm can provide more chances to coalesce. Furthermore, the particles are closely packed in a high-solids-content emulsion, and it can be deduced that under specific RPB hydrodynamic conditions, collision between particles occurs more frequently, and many large-sized particles appear in the RPB emulsification process. The coalescence always occurs between particles that have a large size difference, which means that increasing the emulsification time can boost the occurrence of coalescence. The coalescence and breakup processes compete with each other throughout the emulsification process, beginning with the injection of the pre-polymer into the RPB reactor. Particles are first sheared; then, coalescence takes place, together with breakup, leading to a broader, and even multimodal, PSD. This can be controlled by experimental parameters. Thus, with a suitable high-gravity level and number of cycles, the WPU PSD became broad, enhancing the space utilization and increasing the solids content.

Theoretically, in the preparation of high-solids-content WPU emulsions, viscosity is always a major factor limiting the solids content upper bound. Figure 8(a) reveals the relationship between viscosity and solids content for different emulsions. The viscosity of WPU-STR emulsions grows slowly with a solids content under 45%, but when it reaches the critical point, the viscosity increases sharply. For WPU-RPB, the viscosity remains at a low value until the solids content exceeds 52%. In addition, the increase in the solids content limit shows an advantage of the RPB technology; in general, the interaction between WPU particles is a significant factor influencing the relationship between viscosity and solids content. To simplify this problem, WPU particles are always considered to be rigid spheres, and Brownian movement is identified as the inducement of particle interactions. This implies that at a high solids content, particles collide with others many

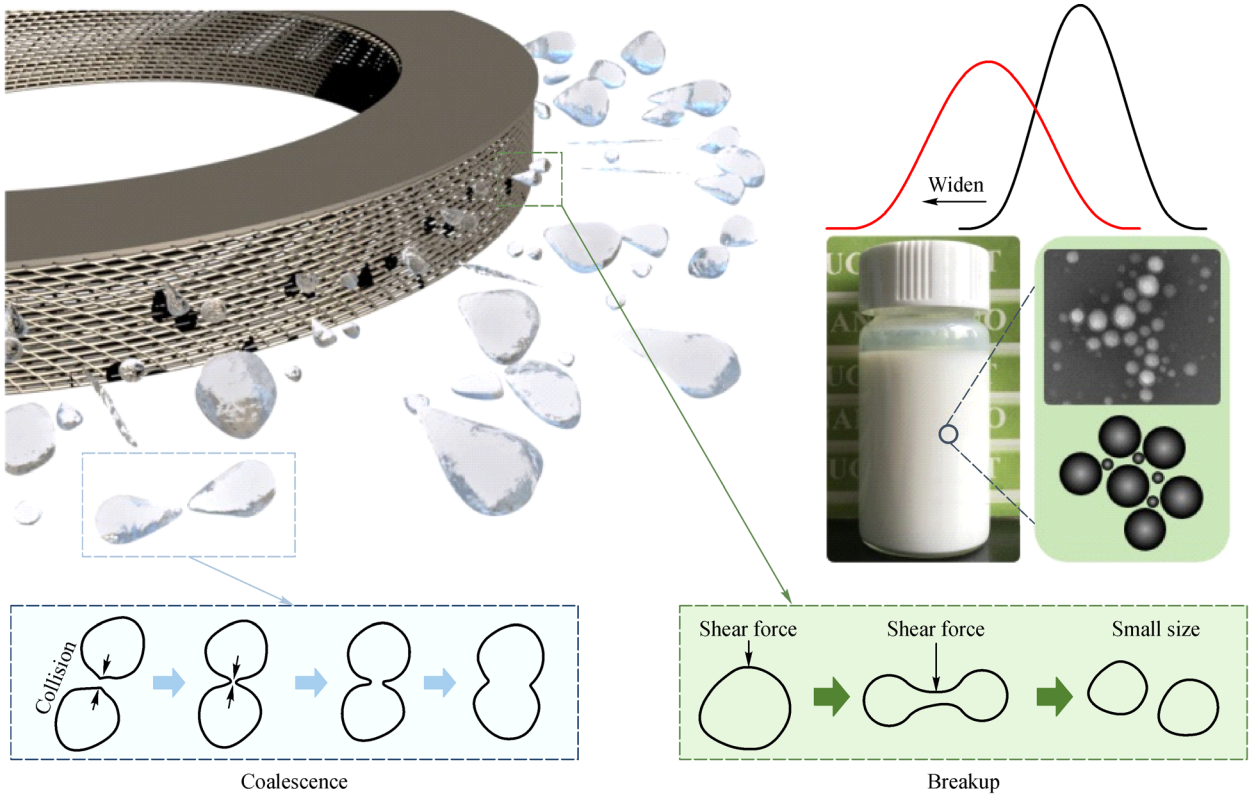

Fig. 7 Schematic diagram of coalescence and breakup in RPB.

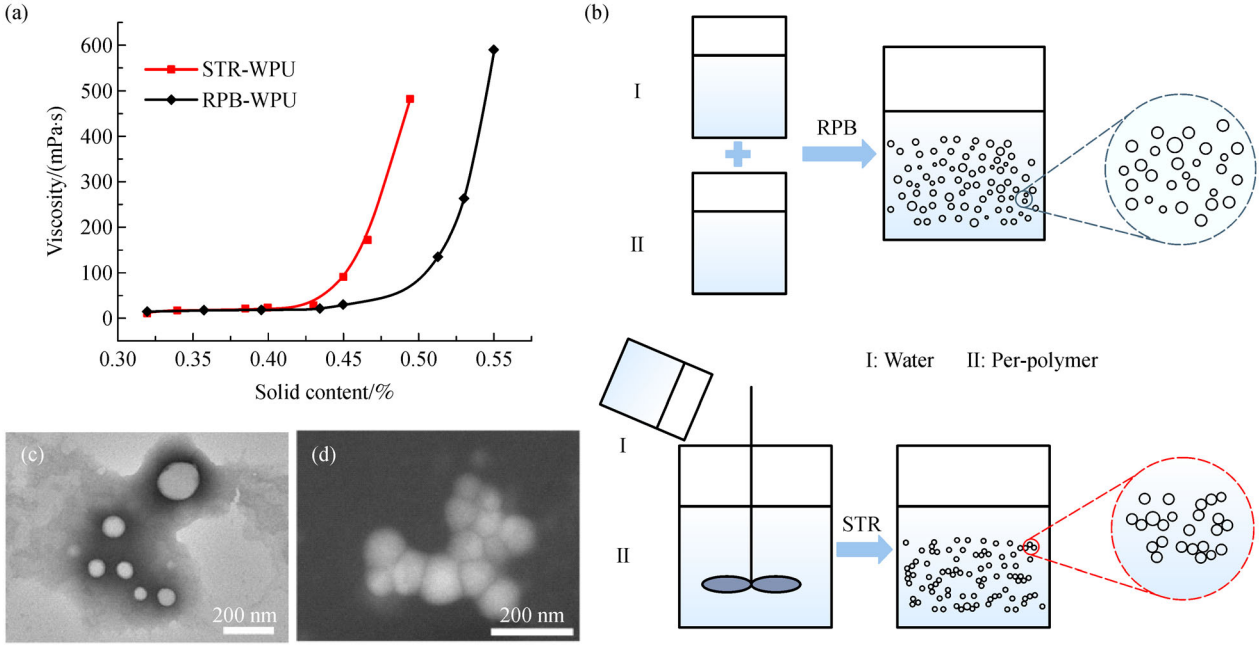

Fig. 8 (a) Relationship between solids content and viscosity of different WPU emulsions; (b) the schematic diagram of different dispersions of emulsions by RPB and STR; (c) TEM morphology of monodisperse particles by RPB; (d) TEM morphology of WPU flocculation.

times and the average distance between WPU particles is small, even close to the hydrodynamic diameter, causing the viscosity to sharply increase. Figure 8(b) is a conceptual figure that shows the difference in particle dispersion between RPB and STR. Under the RPB environment, the WPU pre-polymer passes through the wire mesh packing and is dispersed into a small one, leading to a monodisperse WPU emulsion. Figures 8(c) and 8(d) display TEM images of the WPU particles by RPB and STR, showing the deficiency of STR emulsification. As shown in Fig. 8(a), the STR-WPU emulsion has a higher viscosity at all solids contents compared with RPB-WPU, and the difference is more pronounced at high solids contents. As observed by TEM, the STR-WPU particles underwent marked adhesion, which can be considered a major factor leading to high viscosity. On the contrary, RPB-WPU shows a good monodispersion. This microcosmic phenomenon is the explanation for the macroscopic viscosity, as the dispersity of WPU particles drastically influences the viscosity. In conclusion, a monodisperse nanometer-sized emulsion can be obtained using RPB technology.

Figure 9(a) shows a digital photograph of WPU emulsions prepared at various emulsification times by STR and RPB. As the emulsification proceeds for 20 min, the emulsion obtained using STR was precipitated after a week, which means that emulsification of the pre-polymer was not complete and the successful emulsification time for STR was greater than 20 min. In contrast, the emulsion obtained by RPB can be emulsified in 5 min at least, which indicates that using the RPB reactor is an efficient production strategy. Figure 9(b) shows the effect of WPU coating film with different solids contents (53% and 30%, respectively). The WPU emulsion was white in color, and gradually faded and became transparent during film formation. The WPU films with different solids content had the same drying time, as shown in Fig. 9(c), which shows the relationship between relative weight (%) and drying time of WPU emulsions. The drying rate of WPU coating with high solids content was not significantly improved under the same drying time, but the thickness of WPU films did increase. The thickness of the WPU coating film with 53% solids content was 0.184 mm, and the thickness was 0.095 mm for 30% solids content, as shown in Fig. 9(b). This figure shows the time-saving capacity of the RPB emulsification operation, including a decrease in both emulsification time and drying time because of the increased solids content of the WPU emulsion, which is beneficial for engineering and commercial applications.

In the exploration of the unique microstructure of animal hair, it has been found that the special regular porous microstructure provides the capacity for animals to achieve cold resistance in extreme cold weather, and the bionic structure inspired by animal hair has been considered excellent for thermally insulating materials [36]. The directional freezing process is a new method, which is totally different from the traditional methods of forming pores [37]. The principle of directional freezing is that under a cryogenic environment, ice crystals in a WPU

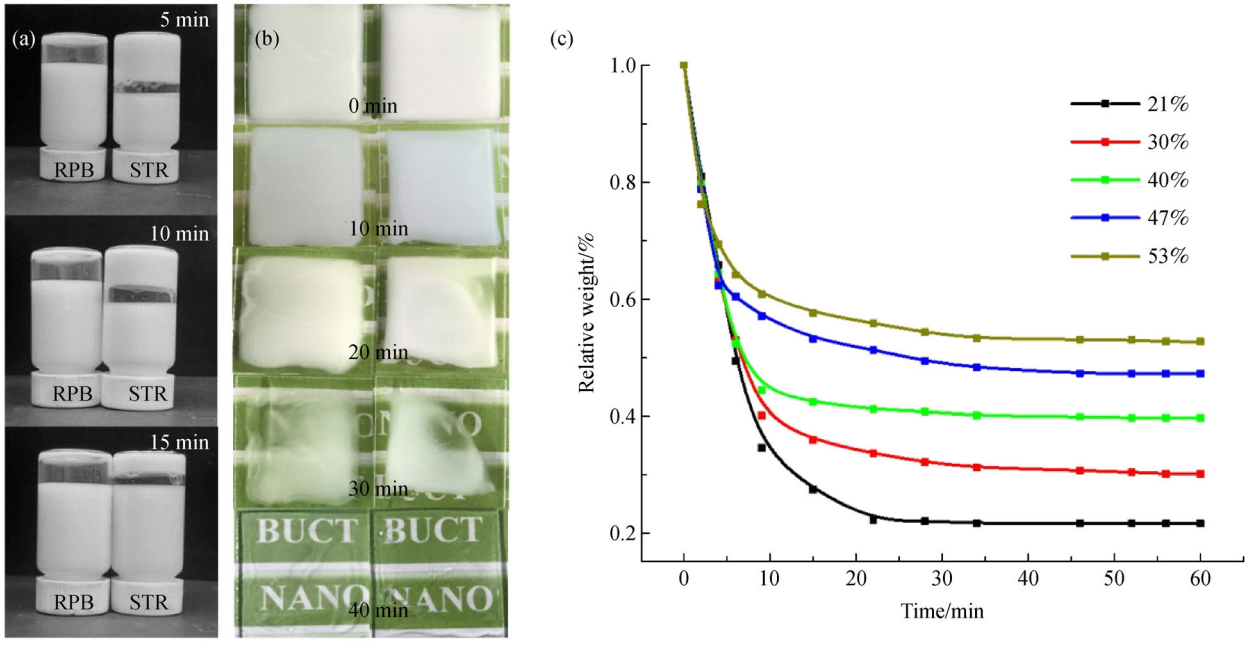

Fig. 9 (a) Digital photograph of WPU emulsion prepared with different emulsification times; (b) two series of digital photographs for WPU coating films with solids contents of 53% and 30% at different times; (c) the relationship between relative weight and time during drying of the WPU coating films.

emulsion would vertically freeze from its bottom surface, which is in contact with a metal disk, to the top surface because of the temperature gradient between the metal disk and the surface. This means that the solids content can control the porosity. In the preparation method, the WPU emulsion sample was configured to have a set solids content. Then, the emulsion was poured into a metal mold and rapidly cooled using liquid nitrogen. After the emulsion froze into a solid, it was moved to the freeze drier to volatilize the solvent for 8 h and obtain the material. In Fig. 10(a), the ambient temperature was kept at 25°C, and a series of infrared images was taken as the heating panel was heated from 50°C to 80°C, where materials prepared with different solids contents and preparation methods were compared. The four samples shown in Fig. 10(a) were prepared under the same freezing conditions; the rounded materials have the same physical dimensions and approximate thicknesses, but showed different thermal insulating performance, which infers that the porous structure was irregular. This was also confirmed by the SEM images. Figure 10(b) shows the WPU material prepared with STR and RPB reactors. Because of the heterogeneity of the WPU system and low solids content, it was difficult to fabricate a material with a stable pore size and uniform pore dispersion. This result means that the emulsion prepared by RPB has a great advantage with respect to preparation of thermal insulation material by a sustainable route. It should be noted that the low-temperature decompression environment required may consume a large amount of energy, which will be a huge barrier to commercialization. However, the material prepared using the RPB reactor can lead to a stable pore size and uniform pore dispersion. This may be a new strategy for production of high-quality WPU thermal insulation material.

Comparing the conventional method and RPB reactor as WPU emulsification devices, regarding the emulsifying mechanism, there is no continuous phase in the RPB emulsification process. Water and WPU were two dispersed phases, which are injected into the packed bed with a set kinetic energy, leading to a balance between breakup and coalescence. In terms of efficiency, the RPB reactor also has a shorter emulsification time, a larger output yield, and the capability of continuous production. In addition, the strong shear force environment of the RPB reactor can also produce a monodispersed emulsion, which has less adhesion, improved stability, and lower viscosity. On the production side, using the RPB reactor can lead to controllable preparation by adjusting operating parameters, which has great significance for the industrial preparation of high-solids-content WPU emulsions. All of these advantages show the superiority of the RPB reactor for WPU emulsification, which means that the high-gravity-assisted emulsification technology has a great potential for use in industrial applications.

4 Conclusions

In summary, we present a two-step continuous production strategy for the preparation of high-solids-content WPU emulsions, using an RPB reactor as an emulsification device. The coalescence of emulsion particles in RPB reactor was proposed to explain the broadening of size distribution, which enhanced the space utilization and increased the solids content. Operation parameters like the pre-polymer flow rate, circulating flow rate, high-gravity level, and number of cycles have been investigated for strengthening of the emulsification process and achieving controllable preparation of particle size and PSD. Favorable dispersibility has also been shown as a result of the strong shear force, which tore WPU droplets into micron to nanometer dimensions, leading to low viscosity and a high solids content. In optimized conditions, we obtained a

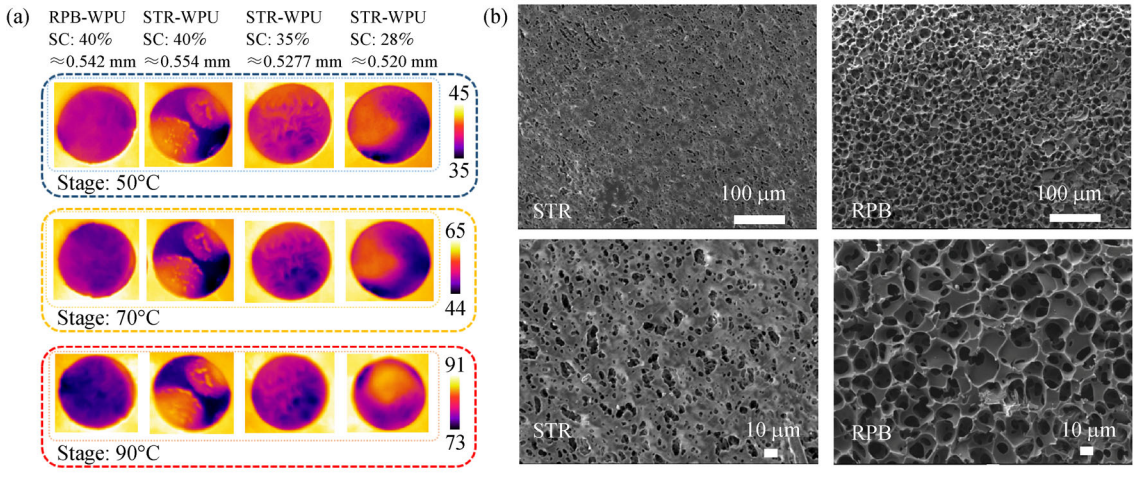

Fig. 10 (a) Infrared images of WPU thermal insulation material with different solids contents and different preparation methods; (b) SEM images of WPU thermal insulation material prepared using STR and RPB reactors.

stable emulsion with a solids content of approximately 55% that had a good emulsion quality. In addition, preliminary applications of high-solids-content WPU for thermal insulating materials were demonstrated.

Acknowledgements This work was supported by the National Key Research and Development Program of China (Grant Nos. 2017YFB-0404302 and 2017YFB0404300).

References

1. Wang S, Du X S, Jiang Y X, Xu J H, Zhou M, Wang H B, Cheng X, Du Z L. Synergetic enhancement of mechanical and fire-resistance performance of waterborne polyurethane by introducing two kinds of phosphorus-nitrogen flame retardant. Journal of Colloid and Interface Science, 2019, 537: 197–205
2. Hu J Q, Peng K M, Guo J S, Shan D Y, Kim G B, Li Q Y, Gerhard E, Zhu L, Tu W P, Lv W Z, et al. Click cross-linking-improved waterborne polymers for environment-friendly coatings and adhesives. ACS Applied Materials & Interfaces, 2016, 8(27): 17499–17510
3. Leng J, Chen J, Wang D, Wang J X, Pu Y, Chen J F. Scalable preparation of Gd_2O_3: Yb^{3+}/Er^{3+} upconversion nanophosphors in a high-gravity rotating packed bed reactor for transparent upconversion luminescent films. Industrial & Engineering Chemistry Research, 2017, 56(28): 7977–7983
4. Yan Q, Dong H, Su J, Han J, Song B, Wei Q, Shi Y. A review of 3D printing technology for medical applications. Engineering, 2018, 4(5): 729–742
5. Yang D J, Wang S Y, Zhong R S, Liu W F, Qiu X Q. Preparation of lignin/TiO_2 nanocomposites and their application in aqueous polyurethane coatings. Frontiers of Chemical Science & Engineering, 2018, 13(1): 59–69
6. Chai C P, Ma Y F, Li G P, Ge Z, Ma S Y, Luo Y J. The preparation of high solid content waterborne polyurethane by special physical blending. Progress in Organic Coatings, 2018, 115: 79–85
7. Chattopadhyay D K, Raju K V S N. Structural engineering of polyurethane coatings for high performance applications. Progress in Polymer Science, 2007, 32(3): 352–418
8. Liang H Y, Wang S W, He H, Wang M Q, Liu L X, Lu J Y, Zhang Y, Zhang C Q. Aqueous anionic polyurethane dispersions from castor oil. Industrial Crops and Products, 2018, 122: 182–189
9. Honarkar H, Barmar M, Barikani M. Synthesis, characterization and properties of waterborne polyurethanes based on two different ionic centers. Fibers and Polymers, 2015, 16(4): 718–725
10. Philipp C, Eschig S. Waterborne polyurethane wood coatings based on rapeseed fatty acid methyl esters. Progress in Organic Coatings, 2012, 74(4): 705–711
11. Feng J, Lu Q H, Tan W M, Chen K Q, Ouyang P K. The influence of the NCO/OH ratio and the 1,6-hexanediol/dimethylol propionic acid molar ratio on the properties of waterborne polyurethane dispersions based on 1,5-pentamethylene diisocyanate. Frontiers of Chemical Science and Engineering, 2019, 13(1): 80–89
12. Król P. Synthesis methods, chemical structures and phase structures of linear polyurethanes. Properties and applications of linear polyurethanes in polyurethane elastomers, copolymers and ionomers. Progress in Materials Science, 2007, 52(6): 915–1015
13. Peng S J, Jin Y, Cheng X F, Sun T B, Qi R, Fan B Z. A new method to synthesize high solid content waterborne polyurethanes by strict control of bimodal particle size distribution. Progress in Organic Coatings, 2015, 86: 1–10
14. Zhou X, Fang C Q, Lei W Q, Du J, Huang T Y, Li Y, Cheng Y L. Various nanoparticle morphologies and surface properties of waterborne polyurethane controlled by water. Scientific Reports, 2016, 6(1): 6
15. Mariz I D A, de la Cal J C, Leiza J R. Control of particle size distribution for the synthesis of small particle size high solids content latexes. Polymer, 2010, 51(18): 4044–4052
16. Mariz I D A, Leiza J R, de la Cal J C. Competitive particle growth: A tool to control the particle size distribution for the synthesis of high solids content low viscosity latexes. Chemical Engineering Journal, 2011, 168(2): 938–946
17. Hou L J, Ding Y T, Zhang Z L, Sun Z S, Shan Z H. Synergistic effect of anionic and nonionic monomers on the synthesis of high solid content waterborne polyurethane. Colloids and Surfaces a-Physicochemical and Engineering Aspects, 2015, 467: 46–56
18. Li M, Liu F, Li Y, Qiang X H. Synthesis of stable cationic waterborne polyurethane with a high solid content: Insight from simulation to experiment. RSC Advances, 2017, 7(22): 13312–13324
19. Lee S K, Kim B K. High solid and high stability waterborne polyurethanes via ionic groups in soft segments and chain termini. Journal of Colloid and Interface Science, 2009, 336(1): 208–214
20. Salager J L, Forgiarini A, Marquez L, Pena A, Pizzino A, Rodriguez M P, Rondo-Gonzalez M. Using emulsion inversion in industrial processes. Advances in Colloid and Interface Science, 2004, 108: 259–272
21. Perazzo A, Preziosi V, Guido S. Phase inversion emulsification: Current understanding and applications. Advances in Colloid and Interface Science, 2015, 222: 581–599
22. Liu H, Hu T, Wang D, Shi J, Zhang J, Wang J X, Pu Y, Chen J F. Preparation of fluorescent waterborne polyurethane nanodispersion by high-gravity miniemulsion polymerization for multifunctional applications. Chemical Engineering and Processing-Process Intensification, 2019, 136: 36–43
23. Wenzel D, Gorak A. Review and analysis of micromixing in rotating packed beds. Chemical Engineering Journal, 2018, 345: 492–506
24. He X, Wang Z, Pu Y, Wan D, Tang R, Cui S, Wang J X, Chen J F. High-gravity-assisted scalable synthesis of zirconia nanodispersion for light emitting diodes encapsulation with enhanced light extraction efficiency. Chemical Engineering Science, 2019, 195: 1–10
25. He X, Tang R, Pu Y, Wang J X, Wang Z, Wang D, Chen J F. High-gravity-hydrolysis approach to transparent nanozirconia/silicone encapsulation materials of light emitting diodes devices for healthy lighting. Nano Energy, 2019, 62: 1–10
26. Wang D, Wang Z, Zhan Q, Pu Y, Wang J X, Foster N R, Dai L. Facile and scalable preparation of fluorescent carbon dots for multifunctional applications. Engineering, 2017, 3(3): 402–408
27. Pu Y, Leng J, Wang D, Wang J X, Foster N R, Chen J F. Process

intensification for scalable synthesis of ytterbium and erbium co-doped sodium yttrium fluoride upconversion nanodispersions. Powder Technology, 2018, 340: 208–216

28. Liu Y, Jiao W, Qi G. Preparation and properties of methanol-diesel oil emulsified fuel under high-gravity environment. Renewable Energy, 2011, 36(5): 1463–1468
29. Modarres-Gheisari S M, Gavagsaz-Ghoachani R, Malaki M, Safarpour P, Zandi M. Ultrasonic nano-emulsification—a review. Ultrasonics Sonochemistry, 2019, 52: 88–105
30. Cui G W, Wang J P, Wang X C, Li W, Zhang X. Preparation and properties of narrowly dispersed polyurethane nanocapsules containing essential oil via phase inversion emulsification. Journal of Agricultural and Food Chemistry, 2018, 66(41): 10799–10807
31. Chen J F, Zhou M Y, Shao L, Wang Y, Yun J, Chew N Y K, Chan H K. Feasibility of preparing nanodrugs by high-gravity reactive precipitation. International Journal of Pharmaceutics, 2004, 269(1): 267–274
32. Wu K, Wu H R, Dai T C, Liu X Z, Chen J F, Le Y. Controlling nucleation and fabricating nanoparticulate formulation of sorafenib using a high-gravity rotating packed bed. Industrial & Engineering Chemistry Research, 2018, 57(6): 1903–1911
33. Kang S Y, Ji Z X, Tseng L F, Turner S A, Villanueva D A, Johnson R, Albano A, Langer R. Design and synthesis of waterborne polyurethanes. Advanced Materials, 2018, 30(18): 1706237
34. Tan C, Lee M C, Abbaspourrad A. Facile synthesis of sustainable high internal phase emulsions by a universal and controllable route. ACS Sustainable Chemistry & Engineering, 2018, 6(12): 16657–16664
35. Guyot A, Chu F, Schneider M, Graillat C, McKenna T F. High solid content latexes. Progress in Polymer Science, 2002, 27(8): 1573–1615
36. Cui Y, Gong H, Wang Y, Li D, Bai H. A thermally insulating textile inspired by polar bear hair. Advanced Materials, 2018, 30(14): 1706807
37. Wu Y J, Xiao C F, Liu H L, Huang Q L. Fabrication and characterization of novel foaming polyurethane hollow fiber membrane. Chinese Journal of Chemical Engineering, 2019, 27(4): 935–943